

Che-Yen Wen,¹ Ph.D.; Shih-Hsuan Chiu,² Ph.D.; Yi-Ren Tseng,² M.S.; and Chuan-Pin Lu,² M.S.

The Mask Detection Technology for Occluded Face Analysis in the Surveillance System

ABSTRACT: The surveillance systems have been widely used in automatic teller machines (ATMs), banks, convenient stores, etc. For example, when a customer uses the ATM, the surveillance systems will record his/her face information. The information will help us understand and trace who withdrew money. However, when criminals use the ATM to withdraw illegal money, they usually block their faces with something (in Taiwan, criminals usually use safety helmets or masks to block their faces). That will degrade the purpose of the surveillance system. In previous work, we already proposed a technology for safety helmet detection. In this paper, we propose a mask detection technology based upon automatic face recognition methods. We use the Gabor filters to generate facial features and utilize geometric analysis algorithms for mask detection. The technology can give an early warning to save-guards when any “customer” or “intruder” blocks his/her face information with a mask. Besides, the technology can assist face detection in the automatic face recognition system. Experimental results show the performance and reliability of the proposed technology.

KEYWORDS: forensic science, mask detection, early warning, surveillance system

The surveillance system has been widely applied in the modern security systems (which are installed in ATMs, banks, convenient stores, etc.). For example, we use the surveillance system of the ATM to record customers’ face information. However, when criminals use the ATM to withdraw illegal money, they usually block their faces with something (in Taiwan, criminals usually use safety helmets or masks to block their faces, Fig. 1). That will degrade the purpose of the surveillance system, such as recognizing the criminals. In previous work, we already proposed a technology for safety helmet detection. The technology can give an early warning to save-guards when any “customer” or “intruder” blocks his/her face information with a safety helmet. In Taiwan, this kind of the safety helmet detection technology will be installed in the surveillance system of ATMs in the near future. We continue the research work and propose a mask detection technology based upon automatic face recognition methods.

The automatic face recognition system is useful for personal identification. The face detection is the kernel technology of the system. Hjelmås, Low (1) and Yang et al. (2) made discussions and gave a good survey on this topic. However, in previous work, researchers gave little attentions to intended occluded face analysis.

In this paper, we propose a robust technology for mask detection. We use the Gabor filters (3–9) to generate facial features and utilize geometric analysis algorithms (10–12) to determine if a mask blocks the face information. This technology can work well on both gray-scale and color images. The technology can give an early warning to save-guards when any “customer” or “intruder” blocks his/her face information with a mask. Besides, the technology can assist the face detection in the automatic face recognition system.

Methods

The proposed mask detection technology is based upon automatic face recognition methods. First, we utilize the Gabor filters (3–9) to generate facial features, and transform the facial features into a binary-block image. Second, we exploit facial feature geometry analytic approaches (Park, et al. (10), Wong, et al. (11) and Jeng, et al. (12)) to analyze the feature blocks and determine if the target person wears a mask. Figure 2 shows the flow chart of the proposed algorithm. The main mask detection algorithm is implemented in the geometric analysis procedure.

Gabor Filters

The Gabor filters are Gaussian-modulated complex sinusoidal functions with three important properties (3–9): (1) they can be designed to be highly selective in frequency while displaying good spatial localization; (2) they resemble the receptive field profiles of the simple cells in the visual pathway; (3) they are band-pass filters, that is, they have tunable orientation and radial frequency bandwidth and tunable center frequency. With those properties, we can use the Gabor filters to extract a specific band of frequency components from an image.

In practice, we utilize the Gabor filters as an operational mask to convolute with the target image. The mathematical model of convolution is described as

$$J_j(\mathbf{x}) = \sum I(\mathbf{x}')\psi_j(\mathbf{x} - \mathbf{x}'), \quad j = 0, \dots, 39, \quad (1)$$

where \mathbf{x} is the coordinate vector, $J_j(\mathbf{x})$ stands for the image after the convolution operation, $I(\mathbf{x})$ stands for the input image, $\psi_j(\mathbf{x})$ stands for the Gabor filters, and

$$\psi_j(\mathbf{x}) = \frac{\|\mathbf{K}_j\|^2}{\sigma^2} \exp\left(-\frac{\|\mathbf{K}_j\|^2 \|\mathbf{x}\|^2}{2\sigma^2}\right) \times \left[\exp(i\mathbf{K}_j \cdot \mathbf{x}) - \exp\left(-\frac{\sigma^2}{2}\right) \right], \quad (2)$$

¹ Department of Forensic Science, Central Police University, Taoyuan, Taiwan.

² Department of Polymer Engineering, National Taiwan University of Science and Technology, Taiwan.

Received 18 Sept. 2004; and in revised form 11 Dec. 2004; accepted 8 Jan. 2005; published 6 April 2005.



FIG. 1—Two real cases in Taiwan. The criminals use the ATM to withdraw illegal money, and they block face information with masks.

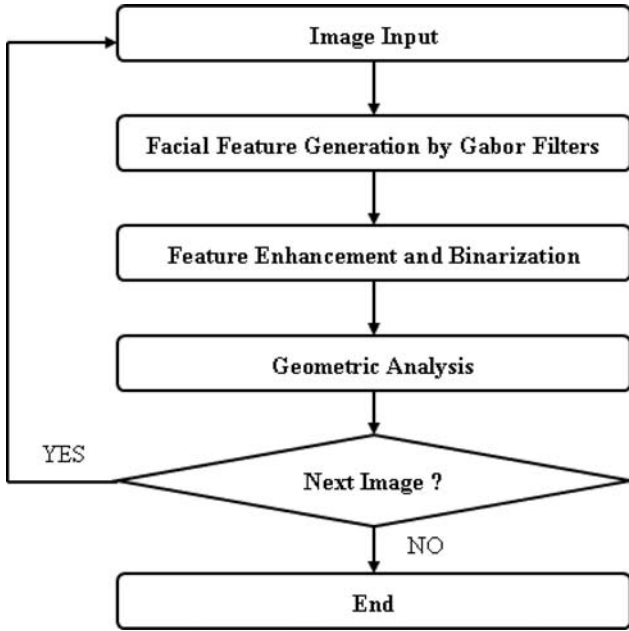


FIG. 2—The flow chart of the method is shown.

where $\|\cdot\|$ stands for the norm-2 operation, i stands for the complex operation and \mathbf{K}_j is the characteristic frequency for each filter, which controls the Gaussian window width, wavelength, and orientation of oscillatory parts. The parameter σ determines the ratio of the window width to the wavelength, (i.e. the number of oscillations under the envelope function). The item $\exp(-\|\mathbf{K}_j\|^2\|\mathbf{x}\|^2/2\sigma^2)$ is the basic Gaussian model and the item $\|\mathbf{K}_j\|^2/\sigma^2$ compensates for the frequency-dependent decrease of the power spectrum in natural images. The item $\exp(i\mathbf{K}_j \cdot \mathbf{x})$ determines the oscillatory part of the kernel. The item $\exp(-\sigma^2/2)$ compensates for the DC-value of the kernel to avoid unwanted dependence of the filter response on the absolute intensity of the image. With high σ values, the effect of DC-term becomes negligible.

$$\mathbf{K}_j = \begin{pmatrix} K_v \cos \varphi_u \\ K_v \sin \varphi_u \end{pmatrix}, \quad K_v = \frac{K_{\max}}{f^v}, \quad \varphi_u = \frac{\pi}{8}u, \quad (3)$$

where $j = u + 8v = 0, \dots, 39$ ($u = 0, \dots, 7$ and $v = 0, 1, \dots, 4$) stands for the frequency of the Gabor filters. K_{\max} is the maximum center frequency, and f is the spacing factor between kernels in the frequency domain. In Fig. 3, we show an example of the

40 feature images generated by the Gabor filters for a facial image. The parameters are $\sigma = \pi$, $f = \sqrt{2}$ and $K_{\max} = \pi/2$.

Feature Enhancement and Binarization

We use a simple non-linear method to enhance the feature images:

$$J'_j(\mathbf{x}) = (J_j(\mathbf{x}))^n \quad (4)$$

where $J'_j(\mathbf{x})$ is the enhanced feature image of $J_j(\mathbf{x})$ (from Eq 1), n is the power order. For the eye blocks and the mouth block analysis, we set $n = 6$ (e.g. Figure 9c is the enhancement result of Fig. 9b) and $n = 3$ (e.g. Figure 10c is the enhancement result of Fig. 10b, respectively).

To simplify the computation, we convert the facial feature image into the binary-block image. We use a simple method to select the threshold values (T_1 and T_2):

$$T_1 = \frac{1}{WH} \sum J'_j(\mathbf{x}), \quad T_2 = 0.5 T_1 \quad (5)$$

where W and H are the width and height of the feature image. We will use T_1 and T_2 in the geometric analysis procedure.

Geometric Analysis

Figure 4 shows the flow chart of the geometric analysis procedure. There are two parts in the procedure: eye and mouth block analysis. The mouth block analysis follows the eye block analysis. In practice, we usually meet the case that the target person wears sunglasses. That is why we need two checking steps in the eye block analysis. One is to find the eye blocks (with the threshold value T_1); the other one is to detect sunglasses (with the second threshold value T_2). We accumulate the energy (intensity or grayscale values) from eight-direction images in the third ($v = 2$, like as Fig. 9b) and first frequency band ($v = 0$, like as Fig. 10b) for the eye and mouth block analysis, respectively.

Eye Block Analysis

We use Fig. 5 to explain the eye block features used in our method. Figure 5a is an original image. Figure 5b is the eye block image obtained by the binarization step. A and B denote the width and height of eyes (we assume both eye blocks have the same width and height), respectively. C denotes the distance between the centers of two eye blocks. We use Eq 6 to compute the block center. In Fig. 6, $O_c(\bar{x}, \bar{y})$ stands for the block center, the coordinates \bar{x} and \bar{y} can be obtained by

$$\bar{x} = \frac{1}{N} \sum_{a=1}^N x_a, \quad \bar{y} = \frac{1}{N} \sum_{a=1}^N y_a, \quad (6)$$

where N is the total pixel number in the block, x_a and y_a are the x and y coordinates of the pixels in the block. The candidate blocks are eye blocks, if they meet the following three conditions:

1. All block centers must lie on their own block regions.
2. $1.0 \leq \frac{A}{B} \leq 1.5$.
3. $1.0 \leq \frac{C}{A} \leq 5.0$.

After locating the eye blocks, we can estimate the slope of the line (i.e. C in Fig. 5b) between two eye blocks. In Fig. 7, we have two eye blocks C_1 and C_2 , C'_1 and C'_2 are their centers, respectively.

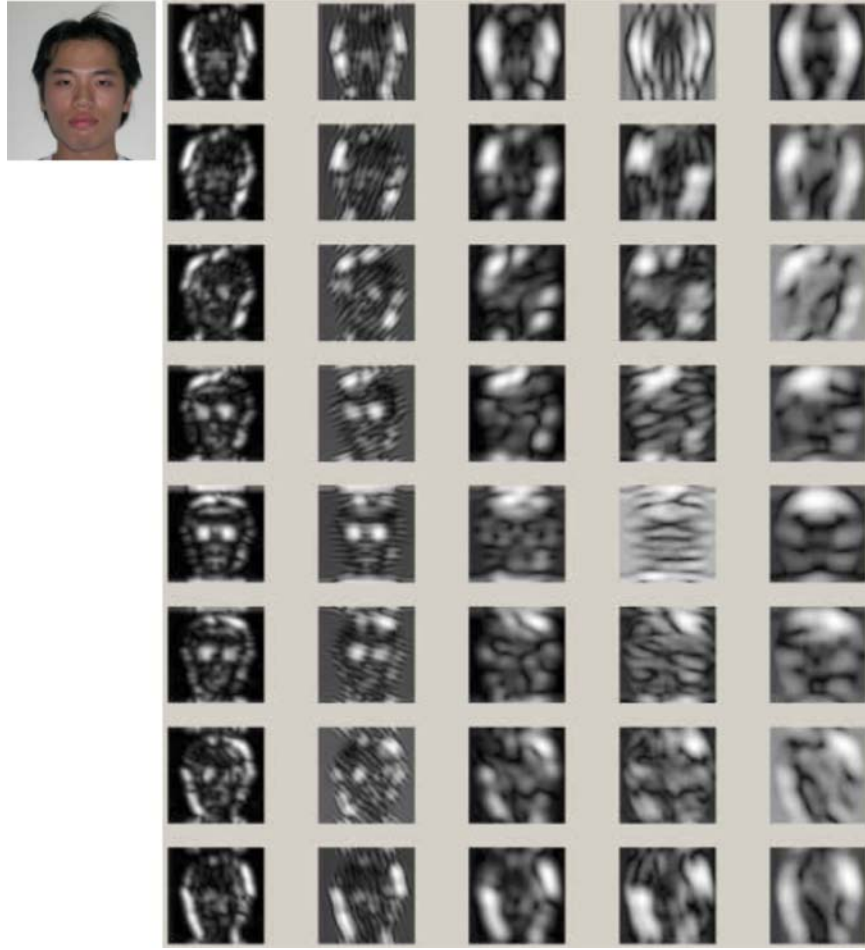


FIG. 3—An example of the response of the Gabor filters with a facial image. The parameters are $\sigma = \pi$, $f = \sqrt{2}$, and $K_{\max} = \pi/2$.

x' denotes the horizontal distance between C'_1 and C'_2 , and the y' denotes the vertical distance between C'_1 and C'_2 . θ_{12} is the line slope and

$$\theta_{12} = \left| \tan^{-1} \frac{y'}{x'} \right| \quad (7)$$

where $|\cdot|$ is the absolute value function.

Mouth Block Analysis

We use Fig. 8 to explain the mouth block features. Figure 8a is an original image. Figure 8b is the block image obtained by the binarization step. D is the distance between two eye block centers (i.e. C in the eye block analysis), E is the distance between the line D and the mouth block. F and G are the mouth block width and height, respectively. The candidate blocks are mouth blocks, if they meet the following five conditions:

1. All block centers must lie on their own block regions.
2. $|O_1 - O_2| \leq 5^0$, where O_1 is the orientation of the mouth block (i.e. the slope of the line F), O_2 is the orientation of the eye blocks (i.e. the slope of the line D).
3. $0.6 \leq \frac{E}{D} \leq 1.5$.
4. $1.0 \leq \frac{F}{G} \leq 4.0$.
5. $0.25 \leq \frac{F}{D} \leq 1.0$.

Experiments

In this section, we show the processes of eye and mouth block analysis. We use synthetic and real images to show the capability of the proposed method.

Demonstration of the Feature Searching and Analysis by Gabor filters

We use Figs. 9 and 10 to show the processes of finding the eye and mouth blocks, respectively.

Figure 9a is the original face image. Figure 9b is the accumulated energy of the eight-direction images of the third frequency band ($v = 2$) in the eye block analysis. Figure 9c is the enhanced result of Fig. 9b ($n = 6$). Figure 9d is the binarization result. Figures 9e and 9f are the results of finding eye blocks.

Figure 10a is the original face image. Figure 10b is the accumulated energy of the eight-direction images of the first frequency band ($v = 0$) in the mouth block analysis. Figure 10c is the enhanced result of Fig. 10b ($n = 3$). Figure 10d is the binarization result. Figures 10e and 10f are the results of finding the mouth block.

Synthetic Image Tests

Figures 11 and 12 show some experimental results of face images without and with masks, respectively. Figures 11a and 12a show the

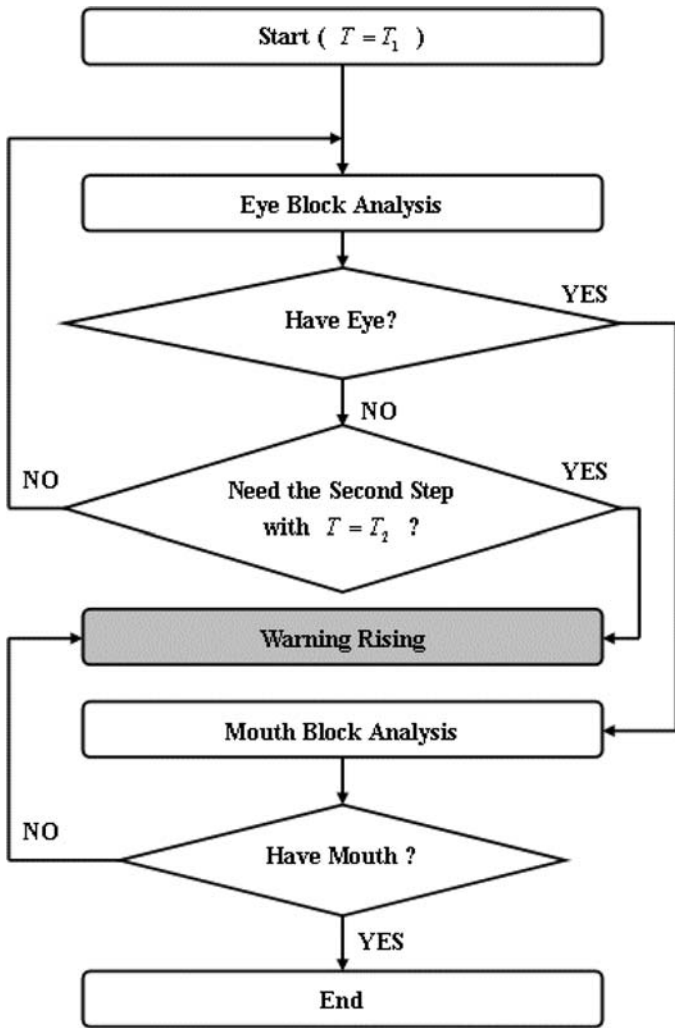


FIG. 4—The flow chart of the geometric analysis procedure.



FIG. 5—The geometric analysis for eye blocks.

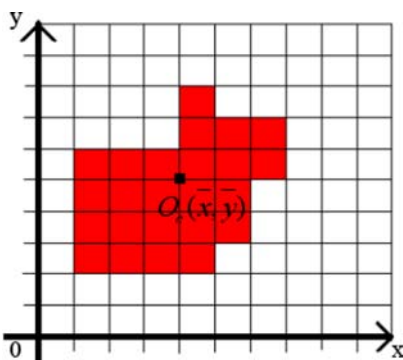


FIG. 6—The center of a block.

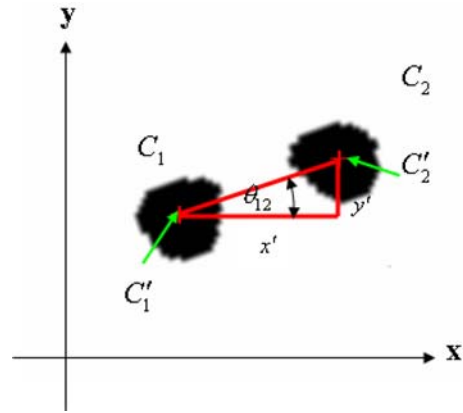


FIG. 7—The line slope (angle θ_{12}) between the two eye blocks.

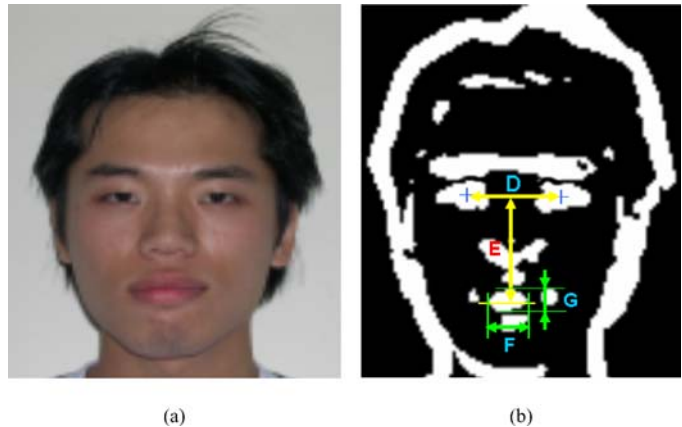


FIG. 8—The geometric analysis for the mouth block.

original face images. Figures 11b and 12b show the mouth blocks. Figures 11c and 12c are the detection results. We use a white block to mark the mouth area if we find the mouth in the image. We show a message “Wearing Mask” when we find a mask in the image.

Figure 13 shows an experimental result of a face image with sunglasses. Figure 13a is the original image. Figures 13b and 13c are the eye and mouth block images, respectively. Figure 13d is the detection result.

Real Image Tests

Figure 14 shows three real cases from the surveillance system. Figure 14a shows the original images. Figure 14b and 14c show the block images and the detection results, respectively.

Conclusions

In this paper, we propose a robust technology for mask detection. We use the Gabor filters to generate facial features and utilize geometric analysis algorithms to determine if a mask blocks the face information. This technology can work well on both gray-scale and color images under controlled environments (e.g., good lighting and image resolutions). The technology can be used to provide an early warning to save-guards when any “customer” or “intruder” blocks his/her face information with a mask. Besides, the technology can assist the face detection in the automatic face recognition system. Experimental results show the performance and reliability of the proposed technology.

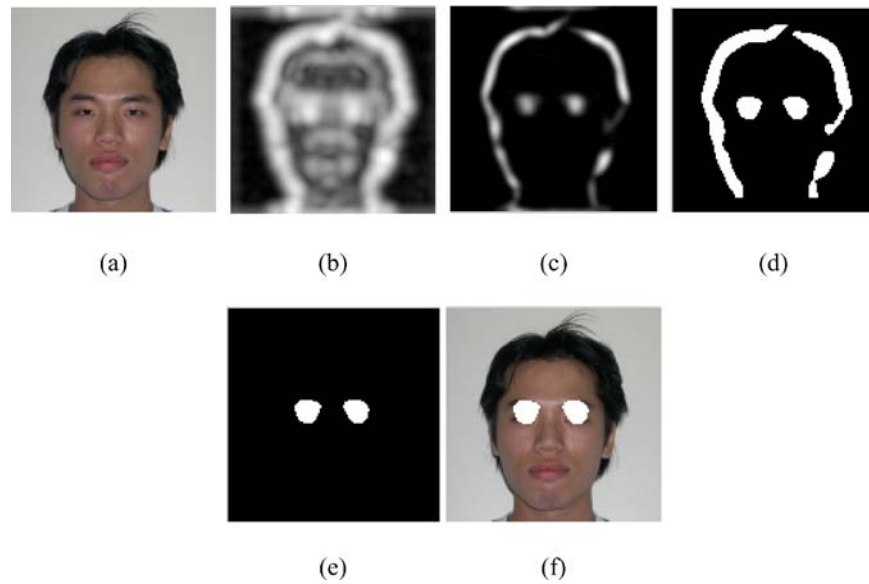


FIG. 9—An example of finding eye blocks: (a) the original face image; (b) the accumulated energy of the eight-direction images of the third frequency band ($v = 2$) in the eye block analysis; (c) the enhanced result of (b) with $n = 6$; (d) the binarization result; (e) and (f) are the results of finding eye blocks.

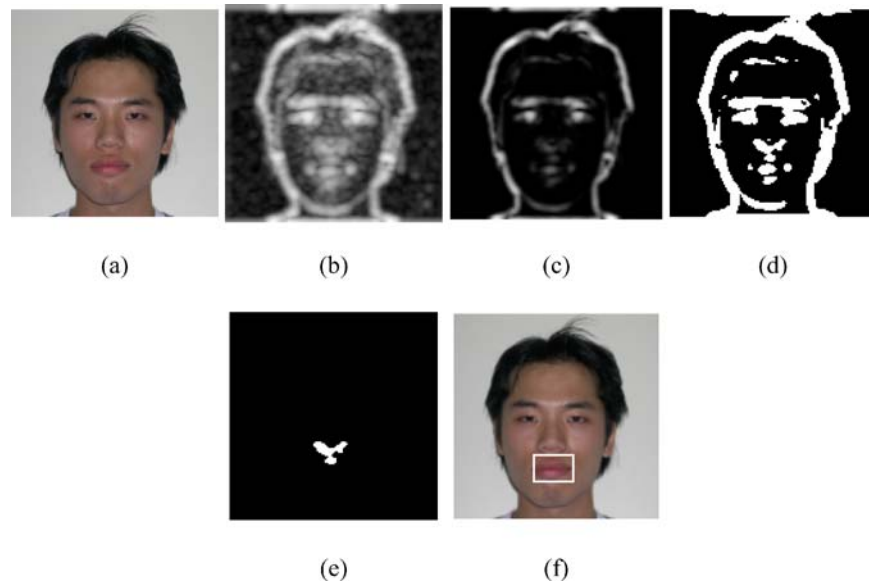


FIG. 10—An example of finding the mouth block: (a) the original face image; (b) the accumulated energy of the eight-direction images of the first frequency band ($v = 0$) in the mouth block analysis; (c) the enhanced result of (b) with $n = 3$; (d) the binarization result; (e) and (f) are the results of finding the mouth block.



FIG. 11—Some experimental results of face images without masks: (a) the original face images; (b) the mouth blocks; (c) the results. We use a white block to mark the mouth area.

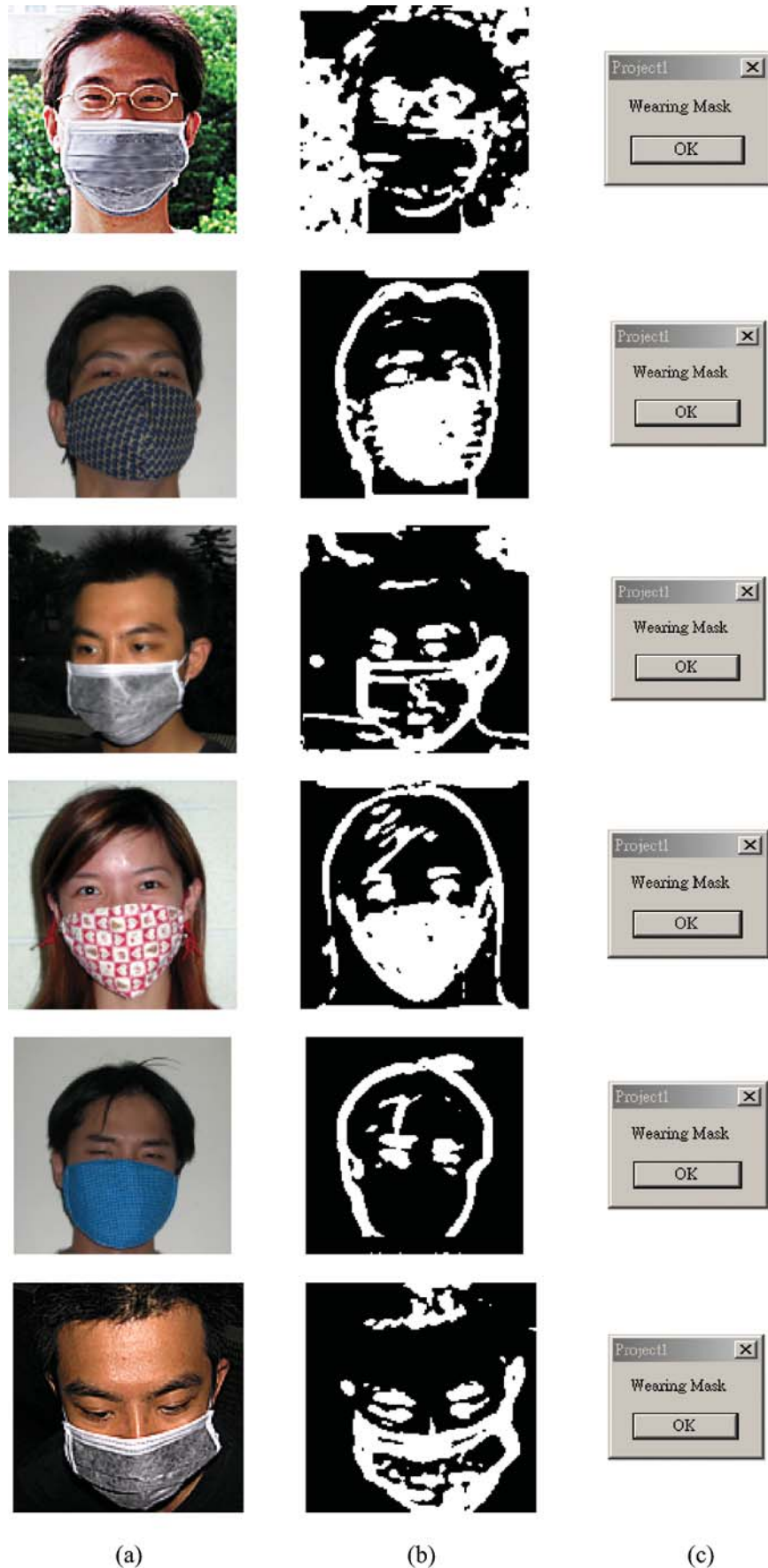


FIG. 12—Some experimental results of face images with masks: (a) the original face images; (b) the mouth blocks; (c) the results. We show a message “Wearing Mask” when we find a mask in the image.

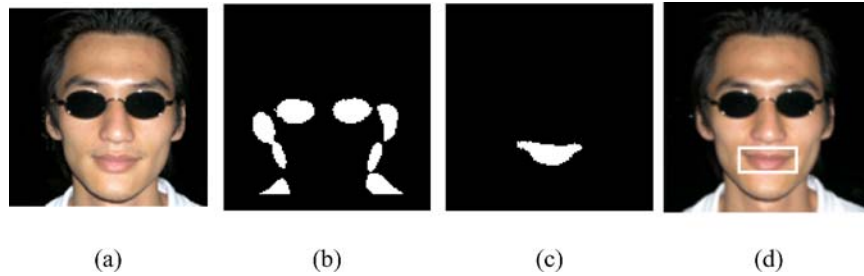


FIG. 13—An experimental result of a face image with sunglasses: (a) the original image; (b) and (c) the eye and mouth block images, respectively; (d) the result.

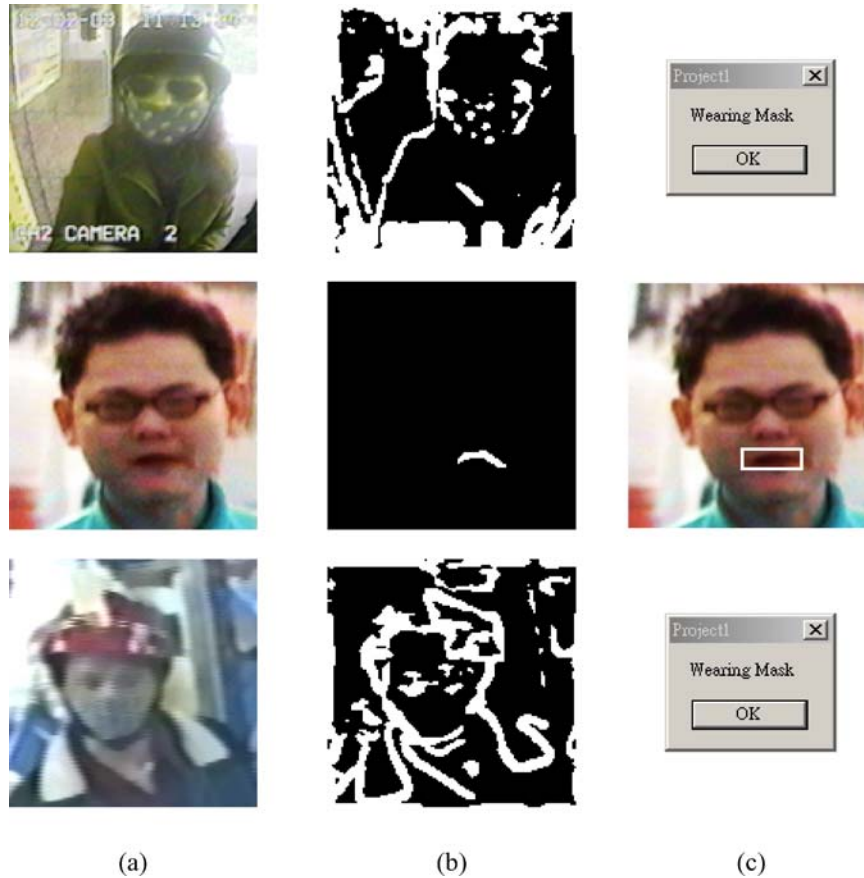


FIG. 14—Real ATMs cases: (a) the original face images; (b) the mouth blocks; (c) the results.

References

- Hjelmås E, Low BK. Face detection: a survey. *Comput Vis and Image Understanding* 2001;83(3):236–74.
- Yang MH, Kriegman DJ, Ahuja N. *Detecting faces in images: a survey*. *IEEE Trans Pattern Anal Machine Intell* 2002;24(1):34–58.
- Kepeñeci B, Tek FB, Akar GB. Occluded face recognition based on Gabor wavelets. *Proceedings of International Conference on Image Processing: 2002 Sep 22–25; Rochester, New York*. New Jersey: The Institute of Electrical and Electronics Engineers, 2002.
- Wang Y, Chua CS, Ho YK, Ren Y. Integrated 2D and 3D images for face recognition. *Proceedings of 11th International Conference on Image analysis and Processing: 2001 Sep 26–28; Palermo, Italy*. California: The IEEE Computer Society, 2001.
- Jain AK, Ratha NK, Lakshmanan S. *Object detection using Gabor filters*. *Pattern Recog* 1997;30(2):295–309.
- Hotta K, Mishima T, Kurita T, Umeyama S. Face matching through information theoretical attention points and its applications to face detection and classification. *Proceedings of 4th IEEE International conference on Automatic Face and Gesture Recognition: 2000 Mar 28–30; Grenoble, France*. California: The IEEE Computer Society, 2000.
- Llanas SC, Garcia JO, Torrico EM, Rodriguez JG. Comparison of feature extraction techniques in automatic face recognition systems for security applications. *Proceedings of IEEE 34th Annual 2000 International Carnahan Conference on Security Technology: 2000 Oct 23–25; Ottawa, Ont. Canada*. New Jersey: The Institute of Electrical and Electronics Engineers, 2000.
- Wang Y, Ho CS, Chua YK. *Facial feature detection and face recognition from 2D and 3D images*. *Pattern Recog Letters* 2002;23(10):1191–202.
- Liu C, Wechsler H. A Gabor feature classifier for face recognition. *Proceedings of 8th IEEE International Conference on Computer Vision*:

- 2001 Jul 7–14; Vancouver, BC Canada. New Jersey: The Institute of Electrical and Electronics Engineers, 2001.
10. Park J, Seo J, An D, Chung S. Detection of human faces using skin color and eyes. IEEE International Conference on Multimedia and Expo: 2000 Jul 30–Aug 2; New York, USA. New Jersey: The Institute of Electrical and Electronics Engineers, 2000.
 11. Wong KW, Lam KM, Siu WC. [An efficient algorithm for human face detection and facial feature extraction under different conditions](#). Pattern Recog 2001;34(10):1993–2004.
 12. Jeng SH, Liao HYM, H CC, Chern MY, Liu YT. [Facial feature detection using geometrical face model: an efficient approach](#). Pattern Recog 1998;31(3):273–82.

Additional information and reprint requests:

Che-Yen Wen, Ph.D.

Department of Forensic Science, Central Police University

56 Shu-Ren Road, Kuei-Shan

Taoyuan, Taiwan 33334

E-mail: cwen@mail.cpu.edu.tw